Progress In Electromagnetics Research M, Vol. 86, 49–57, 2019

Ship Target Tracking Using Underwater Electric Field

Peng Yu*, Jinfang Cheng, and Jiawei Zhang

Abstract—Underwater electric field is an important source of exposure for warship targets, so we try to track the ship's movement by measuring its underwater electric field in this paper. Considering the nonlinear distribution characteristics of underwater electric field, the unscented particle filter method is applied for tracking. First, the equivalent electric field model based on point-electrodes methods is studied. Second, the equivalent electric field model of a scaled ship is used as the electric field source, and the source's movement is tracked by measuring the three components of the underwater electric field induced by the source. To meet the requirements of mine applications, only one measuring node is used in the tracking process. The numerical simulation result shows that the target can be tracked stably within 200 meters of the measuring node. Finally, a sea trail experiment is carried out to examine the effectiveness of this method. In this experiment, the electric field source is composed by two graphite electrodes, and only the horizontal components of underwater electric field are measured. The results show that the tracking performance is good within 150 m of the measuring node.

1. INTRODUCTION

Underwater electric field signals induced by corrosion and anticorrosion currents are important sources of exposure for naval targets, which can be applied to target detection, tracking, and recognition [1, 2]. In shallow water, the electric field signal has better stability than the acoustic signal. In addition, continuous improvements in acoustic stealth make it meaningful for mine weapons, underwater detection nodes and other similar devices to detect or track targets based on the underwater electric field signal [3].

It has been realized to detect ship targets using shaft-rate electric field so far, but the tracking and positioning of ship targets using electric field signals are still in the exploratory stage [4, 5]. For tracking and positioning, the main methods are analytical inversion and filtering estimation. Bao [6] uses the vector information measured by two triaxial electric field sensors to solve the position of the electric dipole source directly. Subsequently, Bao et al. [7] utilize a horizontal electric field sensor array to detect and estimate moving ship targets by using generalized likelihood ratio method. The above two positioning methods both belong to analytical inversion methods which are easily affected by modeling accuracy and environment noise.

At present, the most popular method for moving targets tracking is based on the Bayesian filtering framework. This method regards the target tracking problem as the optimal estimation problem based on Bayesian theory. The main algorithms include Kalman filter, Particle filter and their derivatives. For example, Sun et al. [8] regard the hull as an equivalent electric dipole and applies Extended Kalman Filter (EKF) to track ship's movement for the first time.

As we know, Particle Filter (PF) has obvious advantages over Kalman Filter (KF) in dealing with nonlinear problems. In consideration of the nonlinear characteristics of underwater electric field distribution and propagation, PF is more suitable than KF under this background. Unscented Particle Filter (UPF) is a newly proposed algorithm which has better estimating performance with lower amount

Received 20 May 2019, Accepted 15 September 2019, Scheduled 22 October 2019
* Corresponding author: Peng Yu (15527176627@163.com).
The authors are with the Department of Weaponry Engineering, Naval University of Engineering, 430033, China.

of particle requirements [9, 10]. In the field of image processing, UPF is widely used for target tracking and recognition. In addition, by adjusting the number of particles, UPF algorithm can flexibly adjust between the amount of calculation and the accuracy of estimation.

In this paper, we utilize UPF to track ship's movement. In Section 2, the ship's equivalent electric field model based on point-electrodes method is analyzed. In Section 3, the UPF algorithm is introduced. In Section 4, we use 4 point-electrodes to simulate the electric field of a real ship and use 2 equivalent point-electrodes as the tracking model. The numerical simulation achieves a good performance although some modeling errors exist. In Section 5, a sea trail experiment is carried out to examine the effectiveness of this method.

2. SHIP ELECTRIC FIELD MODELING

Ships have complex structures made of a variety of materials, including different types of carbon steel, low alloy steel, cast steel, copper alloy, aluminum alloy, stainless steel, and titanium alloy. Since these metals' potentials in seawater are different, a primary battery or an electrolytic coupled circuit will be formed when different metals are electrically connected, thus generating electric current in the seawater [11]. For underwater electric field modeling, the hull can be equivalent to many point-electrodes, and the underwater electric field is the result of the interaction of these point-electrodes [12, 13].

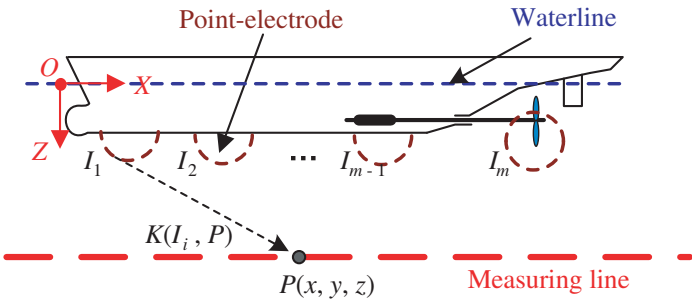

Figure 1. Sketch of ship's underwater electric field modeling based on point-electrodes method.

As shown in Fig. 1, the underwater hull is equivalent to m point-electrodes. The coordinate of each point-electrode i is (x_i, y_i, z_i), and its electric current is $I_i\,(i = 1, ..., m)$. Then the underwater electric potential φ at point $P(x, y, z)$ is the result of the interaction of these point-electrodes [12, 13]:

$$\varphi = \frac{1}{4\pi\sigma_1}\sum_{i=1}^{m} I_i K(i, P) \tag{1}$$

where $K(i, P)$ is a distance function between point P and point-electrode i. In the three-layered homogeneous medium as "air-seawater-seabed", $K(i, P)$ is given by

$$K(i,P) = \frac{1}{\sqrt{r_0^2 + (z - z_i)^2}} + \sum_{n=0}^{\infty}(k)^n\left(\frac{1}{R_1} + \frac{k}{R_2} + \frac{k}{R_3} + \frac{k}{R_4}\right) \tag{2}$$

where

$$\begin{cases} r_0 = (x - x_i)^2 + (y - y_i)^2\,; & k = (\sigma_1 - \sigma_2)/(\sigma_1 + \sigma_2) \\ R_1 = \sqrt{r_0^2 + (z + 2nh + z_i)^2}\,; & R_2 = \sqrt{r_0^2 + (-z + 2(n+1)h - z_i)^2} \\ R_3 = \sqrt{r_0^2 + (z + 2(n+1)h - z_i)^2}\,; & R_4 = \sqrt{r_0^2 + (-z + 2(n+1)h + z_i)^2} \end{cases} \tag{3}$$

In the above formula, h is the depth of seawater; k is the seafloor reflection coefficient; σ_1, σ_2 are the conductivities of seawater and seabed, respectively; n is the number of layers reflected, and the maximum of n could be $10 \sim 20$ in actual engineering [14].

From the above analysis, the modeling of the ship's electric field mainly depends on solving the total number, positions, and electric current values of these equivalent point-electrodes. By measuring the electric field of a known depth underwater, combined with the physical characteristics of the hull, the number, positions, and current values of these equivalent point-electrodes can be solved by the least squares method [15].

3. THE UNSCENTED PARTICLE FILTER

Particle Filter (PF) is also called Sequential Monte Carlo method whose core is to achieve state distribution by extracting random state particles from posterior probability. When performing particle filtering, the proposed distribution or importance distribution of particles is critical. The proposed distribution chosen by the classical particle filtering algorithm is transition probability density, i.e., $q(x_k|X_{k-1}, Y_k) = p(x_k|x_{k-1})$ [16]. It can be seen that this method does not incorporate the latest observation information y_k, resulting in poor estimation.

The UPF algorithm uses the UKF (Unsecured Kalman Filter) algorithm to incorporate the latest observation information and generates a particle distribution that is closer to the true posterior probability. This method greatly reduces the number of particles required and can control the filtering accuracy by adjusting the number of particles. In theory, as the number of particles increases, the estimated states can be infinitely close to the true ones [17].

Based on the modeling method in Section 2, if we assume that a surface ship is combined by two point-electrodes, parameters to be estimated are $[x, y, V_x, V_y, I]$, where (x, y) represents the location of the first point-electrode near the bow; (V_x, V_y) represents the moving speed in x and y direction. I is the current of the first point-electrode near the bow while the current of the other point-electrode is $-I$.

The basic tracking steps of the UPF are as follows [9, 18].

(1) Initialization: When $k = 0$, randomly generate M particles near the initial state variables x_0^i $(i = 1, 2, \cdots, M)$, $x_0^i = [x^i, y^i, V_x^i, V_y^i, I^i]$, according to density function $p(x_0)$, and their weights are $w_0^i = 1/M$. The mean and covariance are

$$\begin{cases} \bar{x}_0^i = E[x_0^i] \\ \mathbf{P}_0^i = E\left[(x_0^i - \bar{x}_0^i)(x_0^i - \bar{x}_0^i)^T\right] \\ \bar{x}_0^{ia} = E[x_0^{ia}] = \left[\,(\bar{x}_0^i)^T \ \mathbf{0} \ \mathbf{0}\,\right]^T \end{cases} \tag{4}$$

Convert the initial covariance to the following matrix form

$$\mathbf{P}_0^{ia} = E\left[(x_0^{ia} - \bar{x}_0^{ia})(x_0^{ia} - \bar{x}_0^{ia})^T\right] = \begin{bmatrix} \mathbf{P}_0^i & 0 & 0 \\ 0 & \mathbf{Q} & 0 \\ 0 & 0 & \mathbf{R} \end{bmatrix} \tag{5}$$

(2) Importance sampling step: At each discrete moment $k = 1 : T$, every particle $i = 1, 2, \cdots, M$ should operate the following steps **a**∼**e**:

a. Generate a set of sigma points for each particle, and the resulting $2L + 1$ sigma points are

$$\chi_{k-1}^{ia} = \left\{\bar{x}_{k-1}^{ia},\ \bar{x}_{k-1}^{ia} \pm \sqrt{(L+\lambda)P_{k-1}^{ia}}\right\} \tag{6}$$

where L is the state dimension; $\lambda = \alpha^2(L+\kappa) - L$; α controls the "size" of the sigma points distribution, generally taken as $0 < \alpha \leq 1$; κ is the scaling parameter, which controls the distance between the sigma points and the state mean, generally taken as $\kappa = 3 - L$.

b. States prediction and covariance matrix update:

States prediction:

$$\begin{cases} \chi_{k|k-1}^{ia} = f(\chi_{k-1}^{ia}) \\ \bar{x}_{k|k-1}^i = \sum_{j=0}^{2L} w_j^m x_{j,\,k|k-1}^i \end{cases} \tag{7}$$

where $f(\cdot)$ represents the state transition, as Equation (19).

Covariance matrix update:

$$\mathbf{P}_{k|k-1}^{i}=\sum_{j=0}^{2L} w_j^c\left(x_{j,k|k-1}^{i}-\bar{x}_{k|k-1}^{i}\right)\left(x_{j,k|k-1}^{i}-\bar{x}_{k|k-1}^{i}\right)^T+Q_k \tag{8}$$

Observations update:

$$\begin{cases}\mathbf{y}_{k|k-1}^{ia}=h(\chi_{k|k-1}^{ia})+v_k\\ \bar{y}_{k|k-1}^{i}=\sum_{j=0}^{2L} w_j^m y_{j,k|k-1}^{i}\end{cases} \tag{9}$$

where Q_k is the state noise; v_k is the observation noise. $h(\cdot)$ represents formula (1), and $\mathbf{y}_{k|k-1}^{ia}$ is the calculated underwater electric potential.

The particle weights are given by Equation (10), where β is the weight control factor of the 0th sigma point, generally $\beta=2$.

$$\begin{cases}w_0^m=\lambda/(L+\lambda)\\ w_0^c=\lambda/(L+\lambda)+(1-\alpha^2+\beta)\\ w_n^m=\lambda/[2(L+\lambda)]\quad n=1,\cdots,2L\end{cases} \tag{10}$$

c. Incorporating the latest observations to solve the Kalman gain and states update:

$$\begin{cases}\mathbf{P}_{y_k y_k}=\sum_{j=0}^{2L} w_j^c\left(y_{j,k|k-1}^{i}-\bar{y}_{k|k-1}^{i}\right)\left(y_{j,k|k-1}^{i}-\bar{y}_{k|k-1}^{i}\right)^T\\ \mathbf{P}_{x_k y_k}=\sum_{j=0}^{2L} w_j^c\left(x_{j,k|k-1}^{i}-\bar{x}_{k|k-1}^{i}\right)\left(y_{j,k|k-1}^{i}-\bar{y}_{k|k-1}^{i}\right)^T\end{cases} \tag{11}$$

Kalman gain:

$$K_k=\mathbf{P}_{x_k y_k}\mathbf{P}_{y_k y_k}^{-1} \tag{12}$$

States update:

$$x_k^i=\bar{x}_{k|k-1}^{i}+K_k\left(y_k-\bar{y}_{k|k-1}^{i}\right) \tag{13}$$

where y_k is the underwater electric potential measured by sensors, while $\bar{y}_{k|k-1}^{i}$ is the estimated electric potential by UPF.

Covariance matrix update:

$$\hat{\mathbf{P}}_k^i=\mathbf{P}_{k|k-1}^{i}-K_k\mathbf{P}_{y_k y_k}K_k^T \tag{14}$$

The importance density function is

$$\hat{x}_k^i=q\left(x_k^i|x_{0:k-1}^i,y_{1:k}\right)=\mathrm{N}\left(\bar{x}_k^i,\hat{\mathbf{P}}_k^i\right) \tag{15}$$

where $N(\cdot)$ is the Gaussian density function.

d. Particle weights calculation and normalization:

$$\hat{w}_k^i\propto\frac{p(y_k|\hat{x}_k^i)p(\hat{x}_k^i|\hat{x}_{k-1}^i)}{q(\hat{x}_k^i|x_{0:k}^i,\,y_{1:k})} \tag{16}$$

Normalization:

$$w_k^i=\hat{w}_k^i\Big/\sum_{i=1}^{M}\hat{w}_k^i \tag{17}$$

e. Resampling and state estimation:

Methods like random weighting, system sampling, residual sampling, etc. can be used to replicate the particles with larger weights, while retaining some particles with smaller weights to ensure that the total number of particles is unchanged.

The final estimated states at moment k are

$$\hat{x}_k = \sum_{i=1}^{M} w_k^i x_k^i \tag{18}$$

When applying the UPF algorithm to the actual electric field tracking, it is necessary to set boundary conditions such as the proper range of velocity and electric dipole moment. When the particle state value exceeds the range, this particle weight is assigned a relatively smaller value in step **e**, which can effectively suppress the states divergence.

4. NUMERICAL SIMULATION

The underwater electric field of ship has strong regional characteristics. For small, medium, and large targets, the effective detection distances are about 200 m, 500 m, and 800 m, respectively. For mine weapons, it is critical to positioning the targets within their attack range (generally no more than 100 m). Therefore, we mainly focus on the tracking performance in the near range of a single measuring node.

4.1. Electric Field Simulation of the Tracked Ship

As it is hard to find a warship for tracking experiment, we use the electric field of a scaled ship model. The scaled ship model is scaled 1 : 50 from a real ship as shown in Fig. 2(a), and the inversion algorithm is used to find the total number, positions, and electric current values of its equivalent point-electrodes according to Section 2. The results show that when the number of point-electrodes is four, the underwater electric field modeling accuracy is no less than 92% at all three depths below the hull as shown in Fig. 2(b). The depths are $1.0B$, $1.5B$, and $2.0B$, where B represents the molded breadth of a ship (molded breadth is the maximum width of a ship).

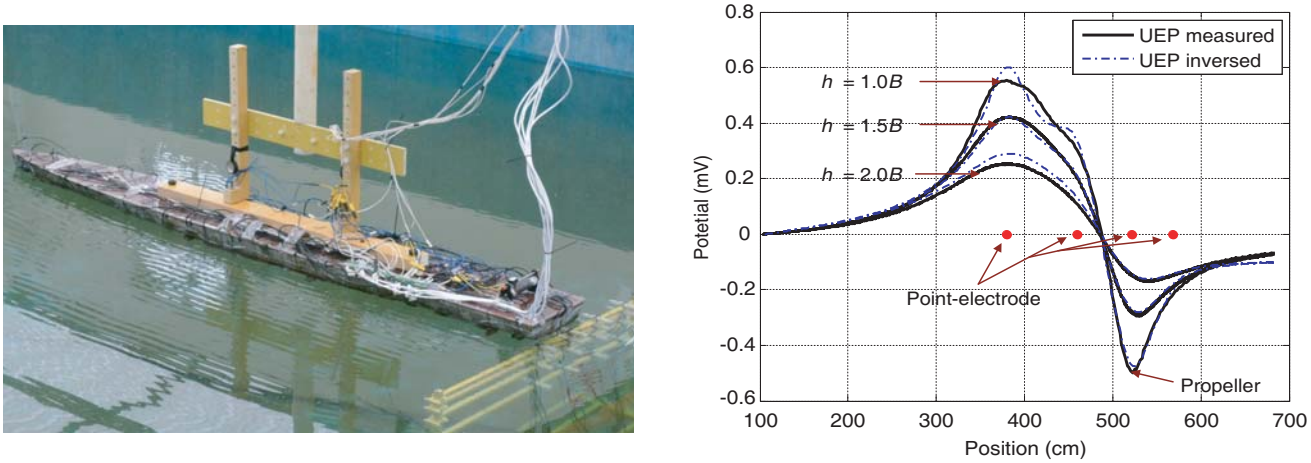

(a) (b)

Figure 2. (a) The scaled ship model whose electric field is used for tracking in numerical simulation; (b) The scaled ship's under water electric field modeling accuracy with 4 point-electrodes.

The positions of these four point-electrodes are all on the keel. The relative positions of these four point-electrodes from the bow to the stern are 0, 79, 141, and 180 (cm), and their current are 3.2, 2.6, -6.5, and 0.4 (mA), respectively.

Now we need to reconstruct the electric field of the real ship. According to the scaling model theory [19, 20], the length and current of the real ship are p and p^2 times of the scaled ship (p is the scaling parameter), respectively. So the positions of the equivalent point-electrodes of the real ship would be 0, 39.5, 70.5, 90 (m), and the corresponding current values are 8.0, 6.5, -16.25, 1.0 (A). Therefore, we use these four point-electrodes to simulate the underwater electric field of a real ship.

4.2. Tracking Model

As we only focus on the tracking performance in the near range, the ship can be assumed to be in line movement with constant velocity. In establishing the tracking model, if we use four point-electrodes to model the target's electric field, the computation will be relatively large, and the tracking results may diverge, although the accuracy of the tracking model is high.

To reduce the computation dimension of the UPF algorithm, the electric field can be equivalent to being generated by two horizontal point-electrodes. It is clear that the modeling accuracy using two point-electrodes is lower than those using four point-electrodes, but it is worth to find a balance between tracking modeling accuracy and computation.

According to Yu et al. [21], the distance between the ship's two equivalent point-electrodes is $1/3 \sim 1/2$ of the ship length. If the distance between these two point-electrodes is set to a certain length within this range, the equivalent electric dipole moment can be estimated accurately by only solving the current values of these two point-electrodes. As a result, the tracking model is established based on two point-electrodes.

(1) State equation:

$$\begin{aligned} X_k &= \Phi X_{k-1} + \Gamma w_{k-1} \\ Y_k &= hX_k + v_k \end{aligned} \tag{19}$$

In the formula, k is the discrete time; X_k is the system state, $X_k = (x_k, y_k, v_k^x, v_k^y, I_k)^T$; x_k, y_k are the coordinates of the ship; v_k^x, v_k^y are the velocities of the target along the x, y direction; I_k is the electric current of the point-electrode, that is, the current of the two point-electrodes are I_k and $-I_k$, respectively; Φ is the state transition matrix; Γ is the state noise coefficient matrix; w_k is the state noise; T is the time interval; $\mathbf{I}$ is Identity matrix.

$$\Phi = \begin{bmatrix} 1 & T & 0 \\ 0 & 1 & T \\ 0 & 0 & \mathbf{I}_{3\times 3} \end{bmatrix}; \quad \Gamma = \begin{bmatrix} 0.5T^2\mathbf{I}_{2\times 2} & 0 & 0 \\ 0 & T\mathbf{I}_{2\times 2} & 0 \\ 0 & 0 & 1 \end{bmatrix}; \quad w_k = \begin{bmatrix} w_k^x & w_k^y & w_k^{vx} & w_k^{vy} & w_k^I \end{bmatrix}^T \tag{20}$$

(2) Observation equation:

According to Equation (1), the electric potential φ_m at a measuring electrode m can be calculated. By calculating the electric potentials of three pairs of measuring electrodes at three different directions, we can get the electric fields E_x, E_y, E_z by the basic equation $E = \Delta\varphi/d$, where $\Delta\varphi$ is the electric potential difference, and d is the distance between two measuring electrodes in x, y, or z direction.

4.3. Tracking Results

The initial states have a significant impact on the tracking performance, and large errors in initial states may lead to divergence in tracking. In this paper, the initial error in states value is set according to the actual situation. The initial states are set $(x_0, y_0) = (350,\ 430)$ (m), $(v_0^x, v_0^y) = (-5, -2)$ (m/s), $I_0 = 10$ A, states noises $w_k = [2,\ 2,\ 0.1,\ 0.1,\ 0.2]^T$, and the number of particles is 50.

In this paper, we define the distance as the horizontal line distance. It can be seen in Fig. 3(b) that the tracking trajectory starts to approach the real trajectory when the line distance is 400 m from the observation point. At this moment, the SNR (Signal to noise ratio) is about 18 dB calculated from Fig. 3(a). When the target is 250 m from the measuring node, the tracking trajectory coincides with the real one (corresponding to point A in Fig. 3(b)), and the corresponding moment is 110 s in Fig. 3(a).

However, when the target leaves the measuring node about 200 m (corresponding to point B in Fig. 3(b)), the tracking trajectory gradually starts to deviate from the real trajectory. This moment corresponds to 280 s in Fig. 3(a) when the SNR is low. The estimated trajectory deviates from the real trajectory mainly due to two reasons: (1) errors exist in modeling the electric field based on two point-electrodes; (2) as the electric field has strong regional characteristics, the SNR will decrease rapidly when the target passes through the measuring node.

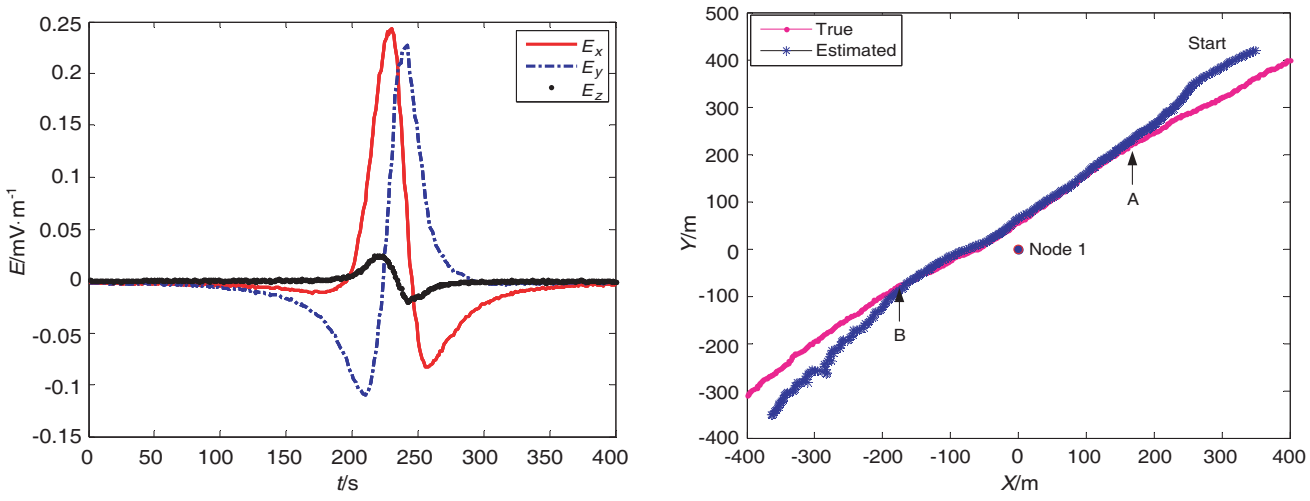

Figure 3. (a) Underwater electric field E_x, E_y, E_z calculated at the measuring mode; (b) Tracking result by UPF; Node 1 represents the location the electric field measuring node.

5. SEA TRAIL EXPERIMENTS

In April 2019, an electric field tracking experiment was carried out in Yantai China. The water depth in the experiment area was 9 m, and the seawater conductivity was 4 S/m. The measuring electrodes were Ag/AgCl electrodes which were fixed on a floating tank as shown in Fig. 4(a). To reduce the influence of sensor position fluctuation, the floating tank was fixed on a floating bridge near the shore as shown in Fig. 4(b), ensuring that the sensor's horizontal movement range did not exceed 0.3 m.

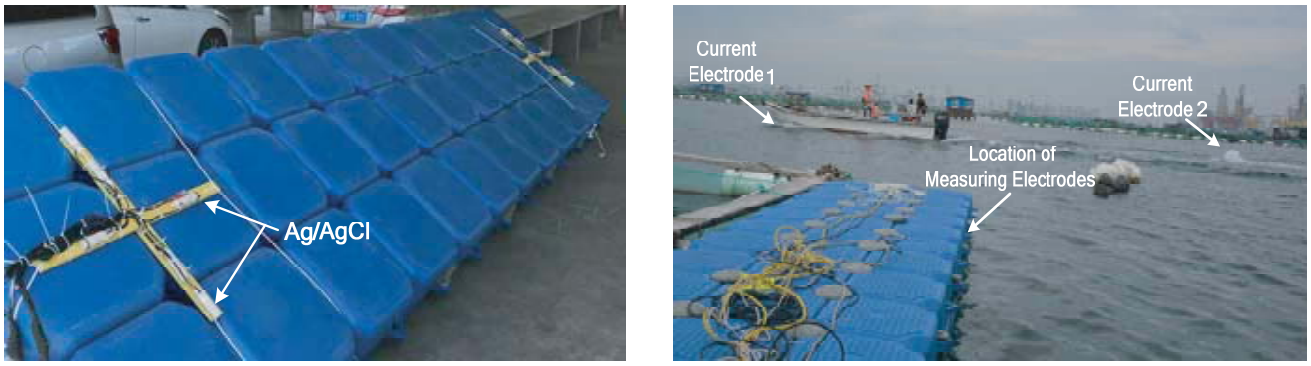

Figure 4. (a) The measuring electrodes are fixed at the bottom of the floating tank and the sea depth of the measuring electrode is 0.2 m; (b) The two current electrodes are towed by a boat at 2.4 m/s.

In the experiment, we measure the horizontal component E_x, E_y of the electric field by two pairs of measuring electrodes. Two graphite electrodes are used as the electric field source; the horizontal distance between two graphite electrodes is 20 m, and the current is 10 A.

To increase SNR, the electric field source uses a 3 Hz sine wave signal and measured electric field signal will be band-pass filtered firstly. Fig. 5(a) is the signal envelope of the filtered electric field data.

The difference between the sea trail experiment and numerical simulation is that only E_x, E_y were measured during the sea trail experiment. It is noteworthy that the system is observable when the system state variables can be reconstructed from the observations [22]. According to Equation (1),

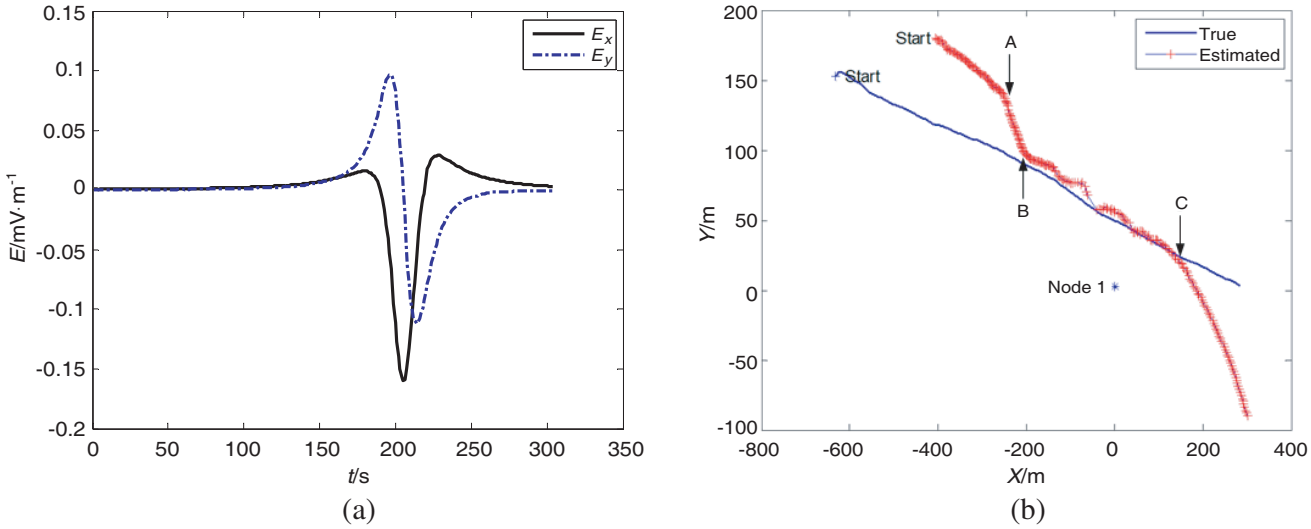

Figure 5. (a) The measured electric field E_x, E_y when the electric field source passed; (b) The tracking results in the sea trial, and Node 1 represented the location of the measuring electrodes.

the underwater electric potential φ is determined by the position x_k, x_k and current I_k of the point-electrodes. So the system is not observable when only E_x, E_y are measured from a single measuring node [20].

Therefore, to make the system observable, current I_k of the point-electrode is regarded as a known parameter in the experiment. As a result, $X_k = (x_k, y_k, v_k^x, v_k^y)^T$.

The tracking result is shown in Fig. 5(b). It can be seen that the estimated trajectory begins to approach the true trajectory when the target is about 280 m from the measuring node (corresponding to point A in Fig. 5(b)). When the target is approaching the measuring node about 220 m, the estimated trajectory coincides with the real one (corresponding to point B in Fig. 5(b)). But the estimated trajectory quickly deviates from the real trajectory when the target is leaving the measuring node about 180 m (corresponding to point C in Fig. 5(b)). Therefore, the effectively tracking time in Fig. 5(b) corresponds to 150 s $\sim$ 270 s in Fig. 5(a). It is clear that the tracking performance highly depends on the SNR of the measured signal although the modeling accuracy is high.

To make the experiment easy to carry out, we place the measuring electrodes on the sea surface, thus making it easier to get the accurate GPS coordinate and attitude angle of these sensors. However, if the sensors were placed on the seabed, the environment noise would be lower, and the location and the attitude angle of the sensor would not change over the flow of the sea. So in the next experiment, the sensor will be placed on the seabed to improve the tracking performance.

6. CONCLUSION

In this paper, UPF algorithm is applied to the ship electric field tracking for the first time. The effectiveness of this method is verified by a numerical simulation and sea trail experiment. Base on a single electric field measuring node, the target trajectory can be effectively tracked within 200 min horizontal line distance. The effective tracking range is closely related to the SNR of underwater electric field signal.

Single measuring node can only achieve close-range tracking. To track and locate the target in a large range, an electric field measuring array is needed, which will be the focus of later research.

ACKNOWLEDGMENT

This work is funded by the research project "Deep Sea of Electromagnetic Detection System", initiated by Pilot National Laboratory for Marine Science and Technology (Qingdao, China).

REFERENCES

1. Lin, C. and S. Gong, *Physical Field of Warships*, 2nd Edition, 233–248, Weapon Industry Press, Beijing, 2007.
2. Marius, B., "Measurement of the extremely low frequency (ELF) magnetic field emission from a ship," *Measurement Science and Technology*, Vol. 22, No. 8, 085709, 2011.
3. Lennartsson, R. K., E. Dalberg, T. Fristedt, et al., "Electric detection of divers in harbor environments," *Oceans*, 1–8, IEEE, 2009.
4. Li, S., C. Zhang, and J. Luan, "Detection of line spectrum of fundamental frequency on shaft-rate electric field of a ship," *ACTA Armamentarii*, Vol. 30, No. 12, 1738–1742, 2009.
5. Jiang, R. and S. Gong, "Vessel's shaft-related electric field signal detection based on the AR model parameter," *Journal of Harbin Engineering University*, Vol. 34, No. 8, 952–956, 2013.
6. Bao, Z., S. Gong, J. Sun, et al., "Localization of a horizontal electric dipole source embedded in deep sea by using two vector-sensors," *Journal of Naval University of Engineering*, Vol. 23, No. 3, 53–57, 2011.
7. Bao, Z., S. Gong, and K. Ma, "Underwater moving target detection and parameter estimation of the array electric field sensor," *Journal of Naval University Of Engineering*, Vol. 27, No. 5, 530–534, 2012.
8. Sun, B.-Q., B. Yan, and R.-X. Jiang, "Application of ship static electric field in ship tracking and positioning," *Journal of Unmanned Undersea Systems*, Vol. 1, 57–62, 2018.
9. Van Der Merwe, R., A. Doucet, N. De Freitas, et al., "The unscented particle filter," *International Conference on Neural Information Processing Systems*, 2000.
10. Wan, E. A. and V. D. M. Rudolph, *The Unscented Kalman Filter*, Kalman Filtering and Neural Networks, 2002.
11. Wu, M., *Cathodic Protection and Anodic Protection*, China Petrochemical Press, Beijing, 2007.
12. Liu, Z. and S. Gong, "Point-electric model of electric field of steady current in sea," *Journal of Naval University of Engineering*, Vol. 16, No. 1, 35–39, 2004.
13. Liu, Z. and W. Wen, *Anti-mine Physical Field Countermeasures Technology*, 154–187, Weapon Industry Press, Beijing, 2015.
14. Jiang, R., C. Lin, and S. Gong, "Electrostatic electric field inversion method for ship based on point charge source model," *Acta Armamentarii*, Vol. 36, No. 3, 545–551, 2015.
15. Yu, P., J.-F. Cheng, and R.-X. Jiang, "Inversion of UEP signatures induced by ships based on PSO method," *Defence Technology*, 2019.
16. Smith, A., *Sequential Monte Carlo Methods in Practice*, Springer Science & Business Media, 2013.
17. Cui, Y. and R. Kavasseri, "Particle filter for dynamic state estimation in multi-machine systems with detailed models," *IEEE Trans. on Power Systems*, Vol. 30, No. 6, 1–9, 2015.
18. Xie, C., Y. Fei, C. Zeng, et al., "State-of-charge estimation of lithium-ion battery using unscented particle filter in vehicle," *Transactions of China Electrotechnical Society*, Vol. 33, No. 17, 3958–3964, 2018.
19. Wang, Y. and K. J. Karis Allen, "Comparison of impressed current cathodic protection numerical modeling results with physical scale modeling data," *Corrosion*, Vol. 66, No. 10, 105001, 2010.
20. Zhou, Y., P. C. Yip, and H. Leung, "Tracking the direction of arrival of multiple moving targets by passive arrays: Algorithm," *IEEE Trans. on Signal Processing*, Vol. 47, No. 10, 2655–2666, 1999.
21. Yu, P., J. Cheng, and R. Jiang, "Research of ship's stealth methods in static electric field," *Advances in Engineering Research*, Tianjin, 2017
22. Birsan, M., "Unscented particle filter for tracking a magnetic dipole target," *Proceedings of IEEE MTS*, Vol. 1, No. 4, 2005.